

## SHELL SIDE NUMERICAL ANALYSIS OF A SHELL AND TUBE HEAT EXCHANGER CONSIDERING THE EFFECTS OF BAFFLE INCLINATION ANGLE ON FLUID FLOW

by

**Rajagopal THUNDIL KARUPPA RAJ\* and Srikanth GANNE**

School of Mechanical and Building Sciences,  
Vellore Institute of Technology, Vellore, Tamil Nadu, India

Original scientific paper  
DOI: 10.2298/TSCI110330118R

*In this present study, attempts were made to investigate the impacts of various baffle inclination angles on fluid flow and the heat transfer characteristics of a shell-and-tube heat exchanger for three different baffle inclination angles namely 0°, 10°, and 20°. The simulation results for various shell and tube heat exchangers, one with segmental baffles perpendicular to fluid flow and two with segmental baffles inclined to the direction of fluid flow are compared for their performance. The shell side design has been investigated numerically by modeling a small shell-and-tube heat exchanger. The study is concerned with a single shell and single side pass parallel flow heat exchanger. The flow and temperature fields inside the shell are studied using non-commercial computational fluid dynamics software tool ANSYS CFX 12.1. For a given baffle cut of 36%, the heat exchanger performance is investigated by varying mass flow rate and baffle inclination angle. From the computational fluid dynamics simulation results, the shell side outlet temperature, pressure drop, re-circulation near the baffles, optimal mass flow rate and the optimum baffle inclination angle for the given heat exchanger geometry are determined.*

Key words: *shell-and-tube heat exchanger, computational fluid dynamics, conjugate heat transfer, pressure drop, baffle inclination angle*

### Introduction

Heat exchangers have always been an important part to the lifecycle and operation of many systems. A heat exchanger is a device built for efficient heat transfer from one medium to another in order to carry and process energy. Typically one medium is cooled while the other is heated. They are widely used in petroleum refineries, chemical plants, petrochemical plants, natural gas processing, air-conditioning, refrigeration, and automotive applications. One common example of a heat exchanger is the radiator in a car, in which it transfers heat from the water (hot engine-cooling fluid) in the radiator to the air passing through the radiator.

There are two main types of heat exchangers:

- direct contact heat exchanger, where both media between which heat is exchanged are in direct contact with each other, and

---

\* Corresponding author; e-mail: [thundil.rajagopal@vit.ac.in](mailto:thundil.rajagopal@vit.ac.in), [ganne2020@gmail.com](mailto:ganne2020@gmail.com)

- indirect contact heat exchanger, where both media are separated by a wall through which heat is transferred so that they never mix.

A typical heat exchanger, usually for higher pressure applications up to 552 bar, is the shell and tube heat exchanger. Shell and tube type heat exchanger is an indirect contact type heat exchanger as it consists of a series of tubes, through which one of the fluids runs. The shell is a container for the shell fluid. Usually, it is cylindrical in shape with a circular cross-section, although shells of different shapes are used in specific applications. For this particular study E shell is considered, which is generally a one pass shell. E shell is the most commonly used due to its low cost and simplicity, and has the highest log-mean temperature-difference (LMTD) correction factor. Although the tubes may have single or multiple passes, there is one pass on the shell side, while the other fluid flows within the shell over the tubes to be heated or cooled. The tube side and shell side fluids are separated by a tube sheet, [1-3]. The heat exchanger model used in this study is a small sized one, as compared to the main stream, all of the leakage and bypass streams do not exist or are negligible, [4-6]. Baffles are used to support the tubes for structural rigidity, preventing tube vibration and sagging and to divert the flow across the bundle to obtain a higher heat transfer coefficient. Baffle spacing (B) is the centre line distance between two adjacent baffles, [7-9]. Baffle is provided with a cut (Bc) which is expressed as the percentage of the segment height to shell inside diameter. Baffle cut can vary between 15% and 45% of the shell inside diameter, [10-12]. In the present study 36% Bc is considered. In general, conventional shell and tube heat exchangers result in high shell-side pressure drop and formation of re-circulation zones near the baffles. Most of the researches now a day are carried on helical baffles, which give better performance than single segmental baffles but they involve high manufacturing cost, installation cost and maintenance cost. The effectiveness and cost are two important parameters in heat exchanger design. So, In order to improve the thermal performance at a reasonable cost of the shell and tube heat exchanger, baffles in the present study are provided with some inclination in order to maintain a reasonable pressure drop across the exchanger [13].

The complexity with experimental techniques involves quantitative description of flow phenomena using measurements dealing with one quantity at a time for a limited range of problem and operating conditions. Computational fluid dynamics (CFD) is now an established industrial design tool, offering obvious advantages [14]. In this study, a full 360° CFD model of shell and tube heat exchanger is considered. By modeling the geometry as accurately as possible, the flow structure and the temperature distribution inside the shell are obtained.

### Computational modeling and simulation

In this study six baffles are placed along the shell in alternating orientations with cut facing up, cut facing down, cut facing up again *etc.*, in order to create flow paths across the tube bundle. The geometric model is optimized by varying the baffle inclination angle *i. e.*, 0°, 10°, and 20°. The computational modeling involves pre-processing, solving and post-processing. The geometry modeling of shell and tube heat exchanger is explained below.

#### *Geometry modeling*

The model is designed according to TEMA (Tubular Exchanger Manufacturers Association) Standards Gaddis (2007), using Pro/E Wildfire-5 software as shown in fig. 1. Design parameters and fixed geometric parameters have been taken similar to Ozden *et al.* [4], as indicated in tab. 1.

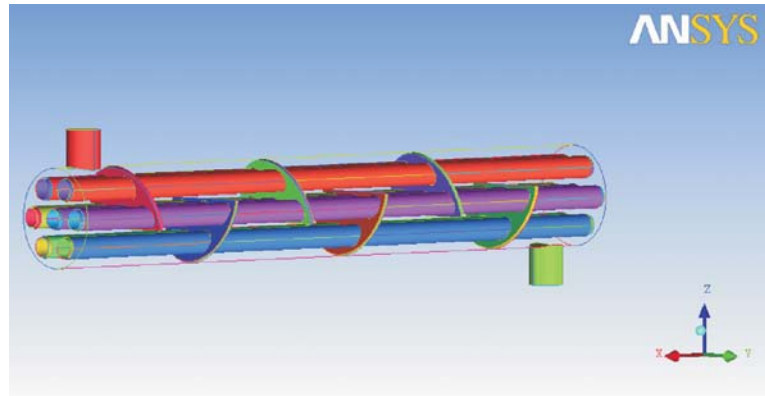


**Figure 1. Isometric view of arrangement of baffles and tubes of shell and tube heat exchanger with 20° baffle inclination**

**Table 1. Geometric dimensions of shell and tube heat exchanger**

Heat exchanger length, $L$	600 mm
Shell inner diameter, $D_i$	90 mm
Tube outer diameter, $d_o$	20 mm
Tube bundle geometry and pitch triangular	30 mm
Number of tubes, $N_t$	7
Number of baffles, $N_b$	6
Central baffle spacing, $B$	86 mm
Baffle inclination angle, $\theta$	0°, 10°, and 20°

### *Grid generation*

The 3-D model is then discretized in ICEM CFD. In order to capture both the thermal and velocity boundary layers the entire model is discretized using hexahedral mesh elements which are accurate and involve less computation effort. Fine control on the hexahedral mesh near the wall surface allows capturing the boundary layer gradient accurately. The entire geometry is divided into three fluid domains Fluid\_Inlet, Fluid\_Shell, and Fluid\_Outlet, and six solid domains namely Solid\_Baffle1 to Solid\_Baffle6 for six baffles, respectively. The heat exchanger is discretized into solid and fluid domains in order to have better control over the number of nodes.

The fluid mesh is made finer than solid mesh for simulating conjugate heat transfer phenomenon. The three fluid domains are as shown in fig. 2. The first cell height in the fluid domain from the tube surface is maintained at 100 microns to capture the velocity and thermal boundary layers. The discretized model is checked for quality and is found to have a minimum

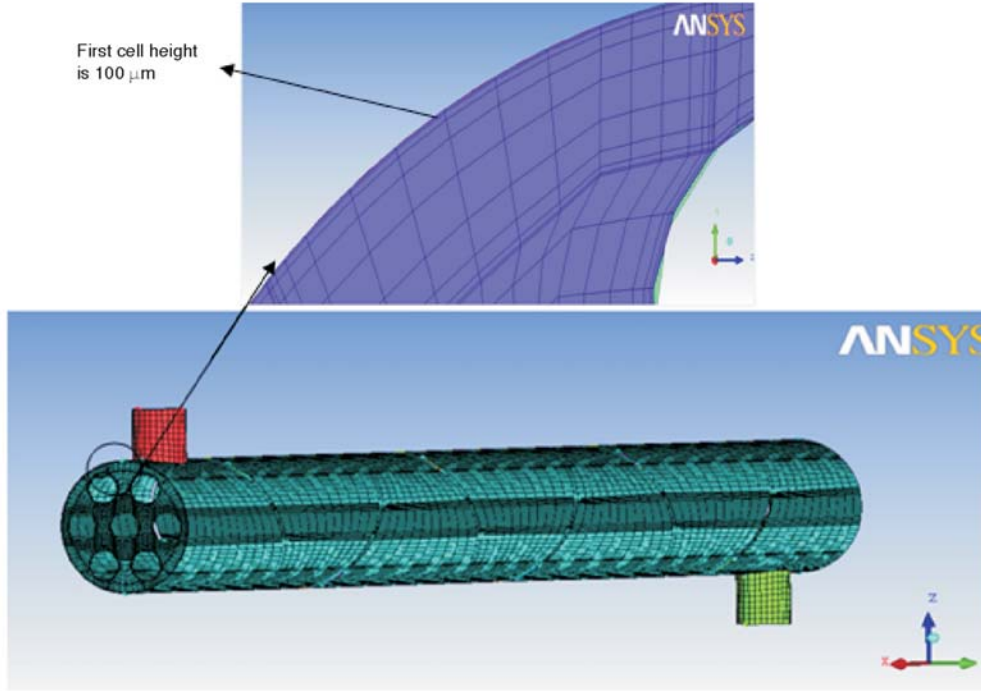


Figure 2. Discretized fluid domain with non-uniform mesh for capturing boundary layer

angle of  $18^\circ$  and min determinant of 4.12. Once the meshes are checked for free of errors and minimum required quality it is exported to ANSYS CFX pre-processor.

### Governing equations

The 3-D flow through the shell-and-tube heat exchanger has been simulated by solving the appropriate governing equations, eq. (1) to eq. (5). viz. conservation of mass, momentum and energy using ANSYS CFX code. Turbulence is taken care by shear stress transport (SST)  $k-\omega$  model of closure which has a blending function that supports Standard  $k-\omega$  near the wall and Standard  $k-\epsilon$  elsewhere.

$$\text{Conservation of mass: } \nabla(\rho\vec{V}) = 0 \quad (1)$$

$$\text{x-momentum: } \nabla(\rho u\vec{V}) = -\frac{\partial p}{\partial x} + \frac{\partial \tau_{xx}}{\partial x} + \frac{\partial \tau_{yx}}{\partial y} + \frac{\partial \tau_{zx}}{\partial z} \quad (2)$$

$$\text{y-momentum: } \nabla(\rho v\vec{V}) = -\frac{\partial p}{\partial y} + \frac{\partial \tau_{xy}}{\partial x} + \frac{\partial \tau_{yy}}{\partial y} + \frac{\partial \tau_{zy}}{\partial z} + \rho g \quad (3)$$

$$\text{z-momentum: } \nabla(\rho w\vec{V}) = -\frac{\partial p}{\partial z} + \frac{\partial \tau_{xz}}{\partial x} + \frac{\partial \tau_{yz}}{\partial y} + \frac{\partial \tau_{zz}}{\partial z} \quad (4)$$

$$\text{Energy: } \nabla(\rho e\vec{V}) = -p\nabla\vec{V} + \nabla(k\nabla T) + q + \phi \quad (5)$$

*Boundary condition set-up*

In ANSYS CFX pre-processor, the various fluid and solid domains are defined. The details of the domains created with the corresponding fluid-solid & fluid-fluid interfaces are provided in tab. 2, respectively. The flow in this study is turbulent, hence SST  $k-\omega$  turbulence model is chosen. The boundary conditions are specified in ANSYS CFX pre-processor and then the file is exported to the ANSYS CFX. The same procedure is adopted for the other two models.

**Table 2. Various domains and interfaces created in ANSYS CFX pre-processor**

Domain location	Domain type	Domain interface	Interface type
FLUID_INLET	Fluid	FLFL_INLET_SHELL	Fluid Fluid
FLUID_OUTLET	Fluid	FLFL_OUTLET_SHELL	Fluid Fluid
FLUID_SHELL	Fluid	FLFL_INLET_SHELL	Fluid Fluid
		FLFL_OUTLET_SHELL	Fluid Fluid
		FLSL_SHELL_BAFFLE1	Fluid Solid
		FLSL_SHELL_BAFFLE2	Fluid Solid
		FLSL_SHELL_BAFFLE3	Fluid Solid
		FLSL_SHELL_BAFFLE4	Fluid Solid
		FLSL_SHELL_BAFFLE5	Fluid Solid
SOLID_BAFFLE1	Solid	FLSL_SHELL_BAFFLE1	Fluid Solid
SOLID_BAFFLE2	Solid	FLSL_SHELL_BAFFLE2	Fluid Solid
SOLID_BAFFLE3	Solid	FLSL_SHELL_BAFFLE3	Fluid Solid
SOLID_BAFFLE4	Solid	FLSL_SHELL_BAFFLE4	Fluid Solid
SOLID_BAFFLE5	Solid	FLSL_SHELL_BAFFLE5	Fluid Solid
SOLID_BAFFLE6	Solid	FLSL_SHELL_BAFFLE6	Fluid Solid

Boundary conditions:

- the working fluid of the shell side is water,
- the shell inlet temperature is set to 300 K,
- the constant wall temperature of 450 K is assigned to the tube walls,
- zero gauge pressure is assigned to the outlet nozzle,
- the inlet velocity profile is assumed to be uniform,
- no slip condition is assigned to all surfaces, and
- The zero heat flux boundary condition is assigned to the shell outer wall (excluding the baffle-shell interfaces), assuming the shell is perfectly insulated.

## Results and discussion

### Validation

Simulation results are obtained for different mass flow rates of shell side fluid ranging from 0.5 kg/s, 1 kg/s, and 2 kg/s. The simulated results for 0.5 kg/s fluid flow rate for model with 0° baffle inclination angle are validated with the data available in [4]. It is found that the exit temperature at the shell outlet is matching with the literature results and the deviation between the two is less than 1%.

The simulation results for 0.5 kg/s mass flow rate for models with 0°, 10°, and 20° baffle inclination are obtained. It is seen that the temperature gradually increases from 300 K at the inlet to 340 K at the outlet of the shell side. The average temperature at the outlet surface is nearly 323 K for all the three models. There is no much variation of temperature for all the three cases considered.

The maximum pressure for models with 0°, 10° and 20° baffle inclinations are 94.43, 91.05, and 79.19 Pa, respectively. The pressure drop is less for 20° baffle inclination compared to other two models due to smoother guidance of the flow. The maximum velocity is nearly equal to 0.302 m/s for all the three models at the inlet and exit surface and the velocity magnitude reduces to zero at the baffles surface. It can be seen that compared to 0° baffle inclination angle, 10°, and 20° baffle inclination angles, provide a smoother flow with the inclined baffles guiding the fluid flow.

From the stream line contour of fig. 3-5, it is found that recirculation near the baffles induces turbulence eddies which would result in more pressure drop for model with  $\theta = 0^\circ$  where as re-circulations are lesser for model with  $\theta = 10^\circ$  and the re-circulations formed for model with  $\theta = 20^\circ$  are much less in comparison to the other two models which indicates the resulting pressure drop is optimum as shown in fig. 6.

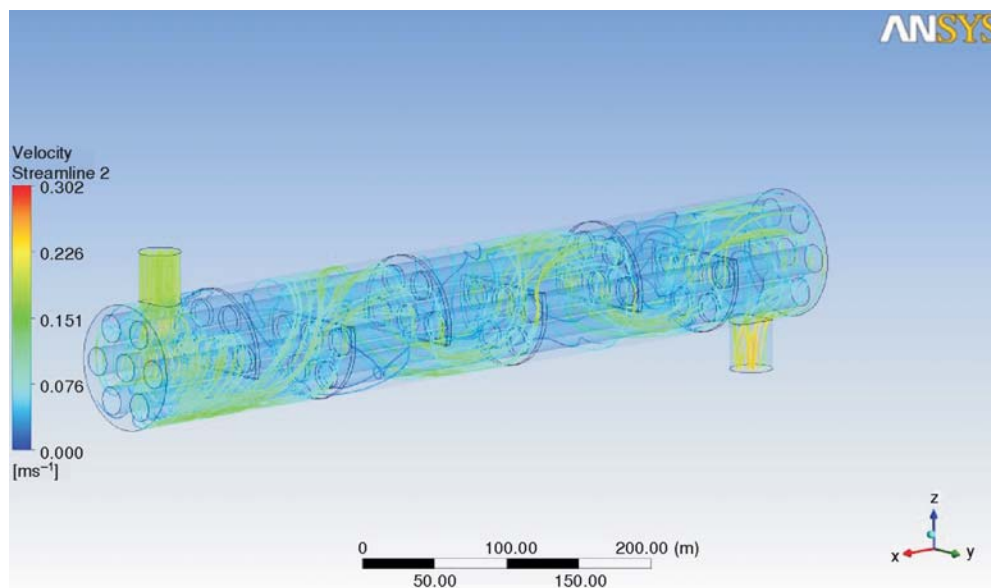


Figure 3. Variation of streamlines along the shell for 0° baffle inclination angle

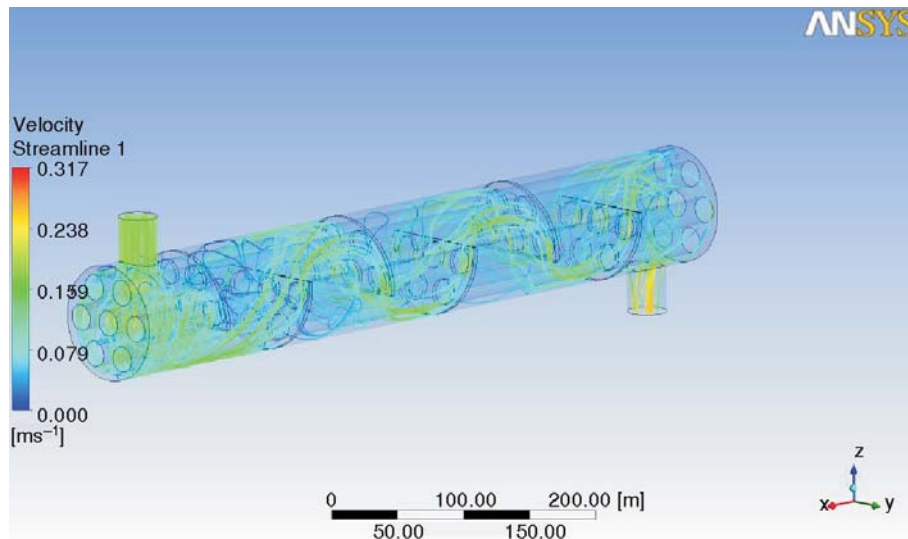


Figure 4. Variation of streamlines along the shell for 10° baffle inclination angle

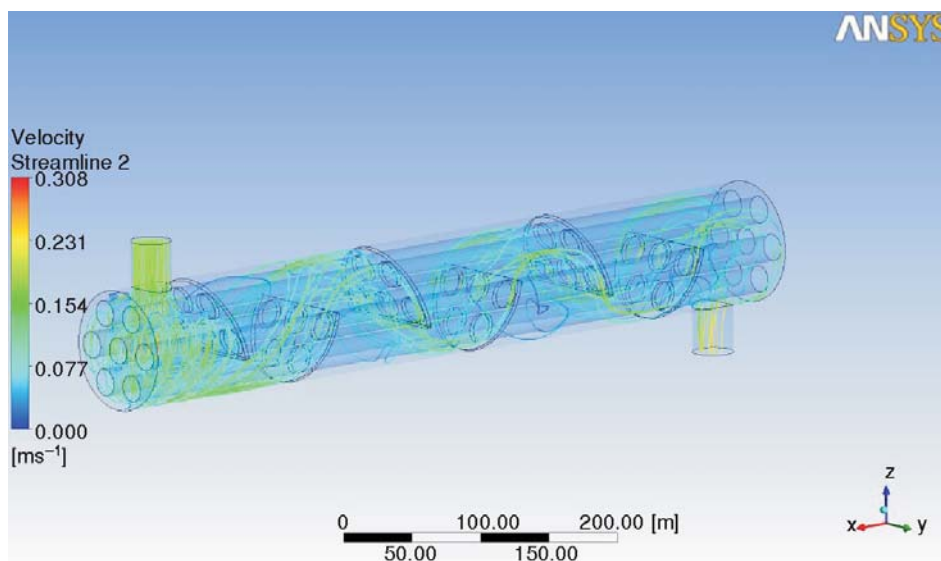


Figure 5. Variation of streamlines along the shell for 20° baffle inclination angle

From the CFD simulation results, for fixed tube wall and shell inlet temperatures, shell side outlet temperature and pressure drop values for varying fluid flow rates are provided in tab. 3 and it is found that the shell outlet temperature decreases with increasing mass flow rates as expected even the variation is minimal as shown in fig. 6. It is found that for three mass flow rates 0.5 kg/s, 1 kg/s, and 2 kg/s there is no much effect on outlet temperature of the shell even



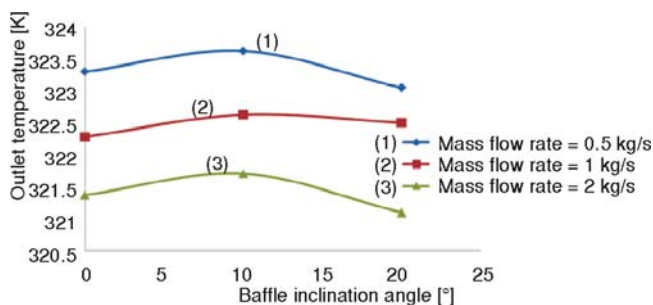


Figure 6. Variation of temperature with baffle inclination angle (for various mass flow rates)

though the baffle inclination is increased from 0° to 20°. However the shell-side pressure drop is decreased with increase in baffle inclination angle *i. e.*, as the inclination angle is increased from 0° to 20°. The pressure drop is decreased by 4 %, for heat exchanger with 10° baffle inclination angle and by 16 % for heat exchanger with 20° baffle inclination compared to 0° baffle inclination heat exchanger as shown in fig. 7. Hence it can be observed that shell and tube heat exchanger with 20° baffle inclination angle results in a reasonable pressure drop. Hence it can be concluded shell and tube heat exchanger with 20° baffle inclination angle results in better performance compared to 10° and 0° inclination angles.

**Conclusions**

Table 3. Outlet temperature and Shell-side pressure drop values for various baffle inclinations and mass flow rates

Baffle inclination angle [degrees]	Mass flow rate = 0.5 kg/s		Mass flow rate = 1 kg/s		Mass flow rate = 2 kg/s	
	Outlet temperature [K]	Pressure difference [Pa]	Outlet temperature [K]	Pressure difference [Pa]	Outlet temperature [K]	Pressure difference [Pa]
0°	323.30	94.43	322.28	377.14	321.37	1507.64
10°	323.62	91.05	322.62	362.12	321.70	1459.89

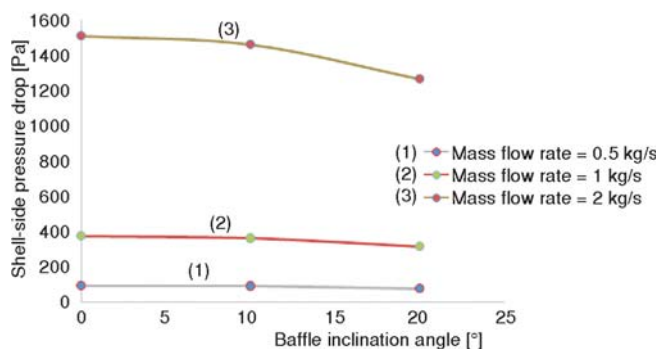


Figure 7. Variation of pressure drop with baffle inclination angle (for mass flow rates of 0.5 kg/s, 1 kg/s, and 2 kg/s)



- The shell side of a small shell-and-tube heat exchanger is modeled with sufficient detail to resolve the flow and temperature fields.
- The shell side of a small shell-and-tube heat exchanger is modeled with sufficient detail to resolve the flow and temperature fields.
- For the given geometry the mass flow rate must be below 2 kg/s, if it is increased beyond 2 kg/s the pressure drop increases rapidly with little variation in outlet temperature.
- The pressure drop is decreased by 4%, for heat exchanger with 10° baffle inclination angle and by 16 %, for heat exchanger with 20° baffle inclination angle.
- The maximum baffle inclination angle can be 20°, if the angle is beyond 20°, the centre row of tubes are not supported. Hence the baffle cannot be used effectively.
- Hence it can be concluded shell and tube heat exchanger with 20° baffle inclination angle results in better performance compared to 10° and 0° inclination angles.

## Nomenclature

$B$	– central baffle spacing, [mm]
$B_c$	– baffle cut, [%]
$D_i$	– shell inner diameter, [mm]
$d_o$	– tube outer diameter, [mm]
$k$	– heat conductivity, [ $\text{Wm}^{-1}\text{K}^{-1}$ ]
$L$	– heat exchanger length, [mm]
$N_b$	– number of baffles, [-]
$N_t$	– number of tubes, [-]
$q$	– heat flux as a source term, [ $\text{Wm}^{-2}$ ]
$T$	– temperature, [K]

$u, v, w$	– velocity components, [ $\text{ms}^{-1}$ ]
$\vec{V}$	– velocity vector, [-]
$x, y, z$	– position co-ordinates, [-]

### Greek symbols

$\theta$	– baffle inclination angle, [deg.]
$\rho$	– density, [ $\text{kgm}^{-3}$ ]
$\tau$	– shear stress, [ $\text{Nm}^{-2}$ ]
$\phi$	– dissipation function, [-]

## References

- [1] Gaddis, D., Standards of the Tubular Exchanger Manufacturers Association, TEMA Inc, 9<sup>th</sup> ed., Tarrytown, N. Y., USA, 2007
- [2] Schlunder, E. V., Heat Exchanger Design Handbook, Hemisphere Publishing Corp., Bureau of Energy Efficiency, New York, USA, 1983
- [3] Mukherjee, R., Practical Thermal Design of Shell-and-Tube Heat Exchangers, Begell House. Inc., New York, USA, 2004
- [4] Ozden, E., Tari, I., Shell Side CFD Analysis of a Small Shell-and-Tube Heat Exchanger, *Energy Conversion and Management*, 51 (2010), 5, pp. 1004-1014
- [5] Kapale, U. C., Chand, S., Modeling for Shell-Side Pressure Drop for Liquid Flow in Shell-and-Tube Heat Exchanger, *International Journal of Heat and Mass Transfer*, 49 (2006), 3-4, pp. 601-610
- [6] Thirumarimurugan, M., Kannadasan, T., Ramasamy, E., Performance Analysis of Shell and Tube Heat Exchanger Using Miscible System, *American Journal of Applied Sciences*, 5 (2008), 5, pp. 548-552
- [7] Sparrows, E. M., Reifschneider, L. G., Effect of Inter Baffle Spacing on Heat Transfer and Pressure Drop in a Shell-and-Tube Heat Exchanger, *International Journal of Heat and Mass Transfer*, 29 (1986), 11, pp. 1617-1628
- [8] Li, H., Kottke, V., Effect of Baffle Spacing on Pressure Drop and Local Heat Transfer in Shell-and-Tube Heat Exchangers for Staggered Tube Arrangement, *Int. J. Heat Mass Transfer*, 41 (1998), 10, pp. 1303-1311
- [9] Than, S. T. M., Lin, K. A., Mon, M. S., Heat Exchanger Design, *Engineering and Technology*, 46 (2008), 22, pp. 604-611
- [10] Kakac, S., Liu, H., Heat Exchangers Selection, Rating and Thermal Design, 2<sup>nd</sup> ed., CRC press, Washington D. C., 2002, pp. 318-335

- [11] Gay, B., Mackley, N. V., Jenkins, J. D., Shell-Side Heat Transfer in Baffled Cylindrical Shell and Tube Exchangers, *Int. J. Heat Mass Transfer*, 19 (1976), 9, pp. 995-1002
- [12] Emerson, W. H., Shell-Side Pressure Drop and Heat Transfer with Turbulent Flow in Segmentally Baffled Shell-Tube Heat Exchangers, *Int. J. Heat Mass Transfer*, 6 (1963), 8, pp. 649-668
- [13] Yong-Gang Lei, *et al.*, Effects of Baffle Inclination Angle on Flow and Heat Transfer of a Heat Exchanger with Helical Baffles, *Chemical Engineering and Processing*, 47 (2008), 12, pp. 2336-2345
- [14] Versteeg, H. K., Malalasekera, W., An Introduction to Computational Fluid Dynamics: the Finite Volume Method, 1<sup>st</sup> ed., Pearson, Essex, UK, 1995